

EXPERIMENTAL STUDY OF A REAL GAS JET

K. A. Malinovskii

Inzhenerno-Fizicheskii Zhurnal, Vol. 14, No. 4, pp. 593-597, 1968

UDC 532.522

The author has experimentally investigated liquid jets propagating in a gas flow at mixing chamber pressures and temperatures of the components such that they may be assumed single-phase.

In engineering, in addition to turbulent gas and liquid jets, one also encounters so-called real gas jets, i. e., jets of gas whose equation of state is essentially different from that of an ideal gas. An example of a real gas jet is a cryogenic liquid flowing from a nozzle into a chamber containing vapors of the same fluid, whose pressure and temperature are higher than the corresponding critical thermodynamic pressure and temperature. In this case it is impossible to speak of a liquid or vapor in the usual sense, since in all regions of the jet the medium is single-phase.

Jet formation depends on the intense heating of the injected component and turbulent mixing. All the parameters such as density, specific heat, and temperature, vary smoothly over the cross section of the jet. There is no surface tension.

Liquid-nitrogen jets were experimentally and theoretically investigated in [1-4].

A more complicated case occurs when a liquid is injected into the vapor of another substance.

On the basis of phase diagrams obtained experimentally [5], it is possible to establish the critical pressure and temperature above which a binary mixture consisting of the liquid forming the jet and the

vapor into which it is injected will be single-phase at any concentration of the components if thermodynamic equilibrium is established.

In a turbulent jet the binary mixture is remote from thermodynamic equilibrium, at any rate in the initial stage of mixing. In this stage alternating regions, in which now one component and now the other predominates, exist in the jet. At a greater distance from the nozzle exit mixing takes place on a smaller scale and at some point reaches the molecular level. In this zone the state of the mixture is close to thermodynamic equilibrium.

If the pressure in the mixing zone and the temperatures of the components are such that there is no surface tension at any point in the boundary layer, and hence no droplets and processes associated with their evaporation, the jet will be single-phase. In this zone the problem of jet propagation can be solved by the ordinary methods of turbulent gas jets [6].

We have investigated jets of Freon-22 and kerosene in a cocurrent flow of gaseous nitrogen heated to 260° C at a pressure of 60 bar. On the basis of phase diagrams of the systems Freon-22-nitrogen and kerosene-nitrogen, obtained at the State Institute of the Nitrogen Industry specially for this purpose, it may be assumed that at the above-mentioned parameters the freon jet is single-phase, whereas the kerosene jet will be two-phase.

Program of Experiments

P, bar	Components	m/sec	kg/m ³	t, °C	$\frac{u_{\infty}}{u_0}$	$\frac{\rho_{\infty}}{\rho_0}$	$\frac{\rho_{\infty} C_{\infty}}{\rho_0 C_0}$																																																																																							
60	Freon-22	17	1215	15	0.65	0.031	0.013																																																																																							
	Nitrogen	11	38	260				60	Kerosene	15	804	15	0.67	0.047	0.02	Nitrogen	10	38	260	40	Nitrogen	20	850	-180	0	0.042	0.023	Nitrogen	0	36	100	Atmospheric pressure	Freon-22	78	2.84	62	0.25	0.039	0.27	Helium	20	0.11	120	Carbon dioxide	65	1.5	106	0.31	0.074	0.44	Helium	20	0.11	120	Freon-22	70	2.84	65	0.28	0.29	0.39	Air	20	0.84	140	Carbon dioxide	70	1.5	96	0.28	0.56	0.64	Air	20	0.84	140	Air	80	1.07	96	0.24	0.79	0.91	Air	20	0.84	140	Helium	80	0.12	107	0.25	6.8	4.3
60	Kerosene	15	804	15	0.67	0.047	0.02																																																																																							
	Nitrogen	10	38	260				40	Nitrogen	20	850	-180	0	0.042	0.023	Nitrogen	0	36	100	Atmospheric pressure	Freon-22	78	2.84	62	0.25	0.039	0.27	Helium	20	0.11	120		Carbon dioxide	65	1.5	106	0.31	0.074	0.44	Helium	20	0.11	120	Freon-22	70	2.84	65	0.28	0.29	0.39	Air	20	0.84	140	Carbon dioxide	70	1.5	96	0.28	0.56	0.64	Air	20	0.84	140	Air	80	1.07	96	0.24	0.79	0.91	Air	20	0.84	140	Helium	80	0.12	107	0.25	6.8	4.3	Air	20	0.84	140							
40	Nitrogen	20	850	-180	0	0.042	0.023																																																																																							
	Nitrogen	0	36	100				Atmospheric pressure	Freon-22	78	2.84	62	0.25	0.039	0.27	Helium	20	0.11	120		Carbon dioxide	65	1.5	106	0.31	0.074	0.44	Helium	20	0.11	120		Freon-22	70	2.84	65	0.28	0.29	0.39	Air	20	0.84	140	Carbon dioxide	70	1.5	96	0.28	0.56	0.64	Air	20	0.84	140	Air	80	1.07	96	0.24	0.79	0.91	Air	20	0.84	140	Helium	80	0.12	107	0.25	6.8	4.3	Air	20	0.84	140																		
Atmospheric pressure	Freon-22	78	2.84	62	0.25	0.039	0.27																																																																																							
	Helium	20	0.11	120					Carbon dioxide	65	1.5	106	0.31	0.074	0.44	Helium	20	0.11	120		Freon-22	70	2.84	65	0.28	0.29	0.39	Air	20	0.84	140		Carbon dioxide	70	1.5	96	0.28	0.56	0.64	Air	20	0.84	140	Air	80	1.07	96	0.24	0.79	0.91	Air	20	0.84	140	Helium	80	0.12	107	0.25	6.8	4.3	Air	20	0.84	140																													
	Carbon dioxide	65	1.5	106	0.31	0.074	0.44																																																																																							
	Helium	20	0.11	120					Freon-22	70	2.84	65	0.28	0.29	0.39	Air	20	0.84	140		Carbon dioxide	70	1.5	96	0.28	0.56	0.64	Air	20	0.84	140		Air	80	1.07	96	0.24	0.79	0.91	Air	20	0.84	140	Helium	80	0.12	107	0.25	6.8	4.3	Air	20	0.84	140																																								
	Freon-22	70	2.84	65	0.28	0.29	0.39																																																																																							
	Air	20	0.84	140					Carbon dioxide	70	1.5	96	0.28	0.56	0.64	Air	20	0.84	140		Air	80	1.07	96	0.24	0.79	0.91	Air	20	0.84	140		Helium	80	0.12	107	0.25	6.8	4.3	Air	20	0.84	140																																																			
	Carbon dioxide	70	1.5	96	0.28	0.56	0.64																																																																																							
	Air	20	0.84	140					Air	80	1.07	96	0.24	0.79	0.91	Air	20	0.84	140		Helium	80	0.12	107	0.25	6.8	4.3	Air	20	0.84	140																																																															
	Air	80	1.07	96	0.24	0.79	0.91																																																																																							
	Air	20	0.84	140					Helium	80	0.12	107	0.25	6.8	4.3	Air	20	0.84	140																																																																											
	Helium	80	0.12	107	0.25	6.8	4.3																																																																																							
	Air	20	0.84	140																																																																																										

Remark. The component above the line forms the jet, subscript 0. The component below the line forms the cocurrent flow, subscript ∞ .

For purposes of comparison, on the same apparatus we investigated heavy and light gas jets in a cocurrent flow at normal pressure.

The program of experiments is summarized in the table, which includes data on liquid-nitrogen jets taken from [3].

The exit diameters of the nozzles forming the jet and the cocurrent flow were respectively equal to 2.5 and 30 mm. Both nozzles were given Vitoshinskii profiles. The nozzle exits were at the same level. During the experiments the total pressure and temperature fields were measured at various distances from the nozzles. The total pressure was measured with a 0.5 mm Pitot tube. The temperature was measured with a chromel-alumel thermocouple, junction diameter 0.4 mm.

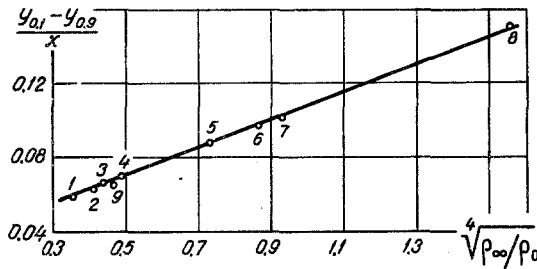


Fig. 1. Effect of density ratio ρ_{∞}/ρ_0 on jet width: 1) Freon-22 jet in nitrogen at P = 60 bar; 2) Freon-22 in helium; 3) kerosene jet in nitrogen at P = 60 bar; 4) carbon dioxide jet in helium; 5) Freon-22 jet in air; 6) carbon dioxide jet in air; 7) air jet in air; 8) helium jet in air; 9) nitrogen jet in nitrogen at P = 40 bar.

Measurements were made at 0.5 mm intervals over the cross section of the jet. Visual observation and photography of the mixing zone were made possible by an IAB-451 shadowgraph. In external appearance real gas jets are similar to shadowgraph pictures of gas jets.

The experiments with gas jets at normal pressure confirmed the known fact that a decrease in the density of the medium leads to a decrease in the expansion angle of the jet and conversely.

Qualitatively, this is also valid for the propagation of a liquid jet in a gas [7].

The experimental data were analyzed using the relations

$$Q = \frac{\Delta(\rho u^2)}{\Delta(\rho u^2)_m} = \frac{\langle \rho u^2 \rangle - (\rho u^2)_{\infty}}{(\rho u^2)_m - (\rho u^2)_{\infty}} = f\left(\frac{y}{x}\right),$$

$$\tau = \frac{\Delta T}{\Delta T_m} = \frac{\langle T \rangle - T_{\infty}}{T_m - T_{\infty}} = f\left(\frac{y}{x}\right).$$

The graphs presented in the figures relate to a distance from the nozzle exit $x = 30$ mm.

If a quantity proportional to the width of the jet is plotted along the ordinate axis and the fourth root of

the density ratio along the axis of abscissas, then all the experimental points lie close to a straight line

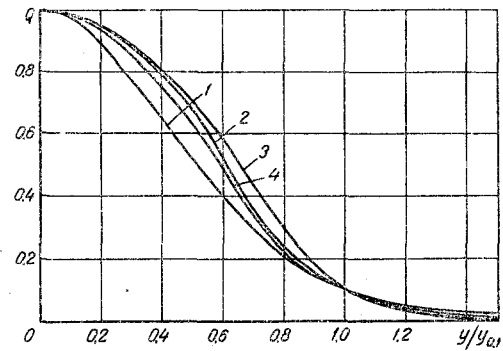


Fig. 2. Dimensionless dynamic pressure profiles in generalized coordinates: 1) gas jet; 2) Freon-22 jet in nitrogen at P = 60 bar; 3) kerosene jet in nitrogen at P = 60 bar; 4) liquid-nitrogen jet in nitrogen at P = 40 bar.

(Fig. 1). On this graph we have also plotted the data of [3] for a liquid-nitrogen jet in a gaseous nitrogen medium at a temperature of 100°C and a pressure of 40 bar.

The graphs shown in Fig. 2 represent ρu^2 in generalized coordinates. The dynamic pressure profiles obtained from experiments with gases at normal pressure coincide. This again confirms the frequently observed fact [8] that the dynamic pressure fields are similar.

The same figure shows the ρu^2 profiles of Freon-22, kerosene, and liquid-nitrogen [3] jets propagating in a cocurrent flow of gaseous nitrogen at high pressure. Clearly, these profiles are not similar to the ρu^2 fields of an ideal gas or to each other. Obviously, the sharp difference in the properties of the substances forming

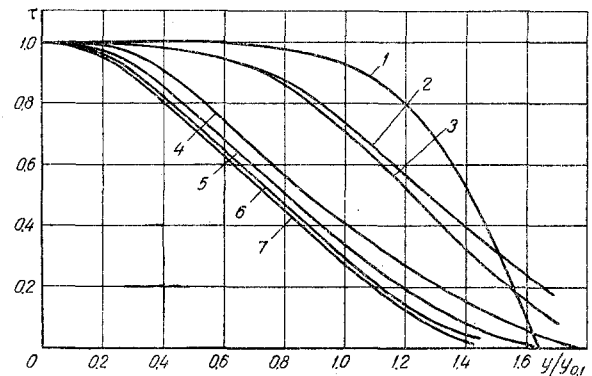


Fig. 3. Dimensionless temperature profiles in generalized coordinates: 1) Freon-22 jet in nitrogen at P = 60 bar; 2) kerosene jet in nitrogen at P = 60 bar; 3) liquid-nitrogen jet in nitrogen at P = 40 bar; 4) Freon-22 jet in helium; 5) Freon-22 jet in air; 6) carbon dioxide jet in air; 7) air jet in air.

the real-gas and ideal-gas jets affects the mixing process, which leads to a difference in the total pressure fields.

If we consider some point of the boundary layer, then from physical considerations we may conclude that its temperature will differ the less from the temperature in the core of the jet, the heavier the jet and the greater the specific heat of the substance forming the jet C_0 . In other words, as the ratio $\rho_\infty C_\infty / \rho_0 C_0$ decreases, the temperature profile should become fuller.

The effect of the parameter $\rho_\infty C_\infty / \rho_0 C_0$ on the temperature profile is illustrated by the experimental data presented in Fig. 3. In this figure the dimensionless temperature profiles have been referred to the distance between the jet axis and the point at which the dynamic pressure is one tenth of the dynamic pressure on the axis.

Clearly, the temperature profiles of Freon-22, kerosene, and liquid nitrogen are much broader than the temperature profiles of the gas jets. Correspondingly, the parameter $\rho_\infty C_\infty / \rho_0 C_0$ for Freon-22, kerosene, and liquid-nitrogen jets is an order less than for the gas jets. It may be assumed that the gas jet temperature profiles also have a tendency to arrange themselves in the same order, but this requires further experimental verification.

NOTATION

y is the distance from jet axis; x is the distance from nozzle exit; u is the velocity component in x direction; ρ_∞ is the density of substance in cocurrent flow; ρ_0 is the density of substance forming jet; $\langle \rho u^2 \rangle$ is the averaged dynamic pressure at measuring point; $(\rho u^2)_\infty$ is the dynamic pressure of cocurrent flow;

$(\rho u^2)_m$ is the dynamic pressure on jet axis; $\langle T \rangle$ is the averaged temperature at measuring point; T_∞ is the temperature of cocurrent flow; T_m is the temperature on jet axis; $y_{0.1}$ and $y_{0.9}$ are the distances from jet axis to points at which the excess dynamic pressure $\Delta(\rho u^2)$ is respectively 0.1 and 0.9 of the excess dynamic pressure on the axis $\Delta(\rho u^2)_m$; t is the temperature, °C; C is the specific heat at constant pressure; P is pressure, bar.

REFERENCES

1. V. I. Bakulev, *Inzh. zh.*, **1**, no. 3, 1961.
2. V. I. Bakulev, *IFZh*, **7**, no. 10, 1964.
3. G. N. Abramovich, V. I. Bakulev, I. S. Makarov, and B. G. Khudenko, *Izv. AN SSSR, Mekhanika zhidkosti i gaza*, no. 1, 1966.
4. G. N. Abramovich, V. I. Bakulev, V. A. Golubev, and G. G. Smolin, *Int. J. Heat Mass Transfer*, **9**, 1047, 1966.
5. I. R. Krichevskii, *Phase Equilibria in Solutions at High Pressures* [in Russian], Goskhimizdat, 1952.
6. G. N. Abramovich, *Theory of Turbulent Jets* [in Russian], Fizmatgiz, 1960.
7. M. A. Styrikovich and S. S. Kutateladze, *Hydraulics of Gas-Liquid Systems* [in Russian], Gosenergoizdat, 1958.
8. L. A. Vulis and V. L. Kashkarov, *Theory of Viscous-Fluid Jets* [in Russian], *Izd. Nauka*, 1965.

13 July 1967

Ordzhonikidze Aviation Institute, Moscow